Helicopter Rotor Vibration Reliability Control Analysis

Prof. Rafiq A. Kanai, Dr. S. P. Chavan

Abstract-The benefits of applying multiple alternatives for mock-up and compression of helicopter harmonic motion are analyzed. Multiple mock-up approaches, along with a weighted-average mechanism, are approximated so that quicksand affiliated with only applying alone better alternate for the rotor blade vibration-reduction dilemma are bypassed. A harmonic motion external function matching to a flight circumstance in which blade-vortex collaboration drives amplitudinous levels of harmonic motion is accounted. The design variables consist of cross-sectional areas of the architectural component of the blade and non-architectural masses. The optimized considerations are matched with a baseline consideration looking like a UF-60 reference blade. The aftereffects demonstrate that at relatively insufficient additional cost matched with optimizing a single alternate, multiple alternates can be applied to connect diverse reduced-vibration concepts that would be excused if only a single mock-up method was exercised, and the most precise alternate may not control to the superior design.

Index Terms— Rotor harmonic motion, air carrier, vibration analysis, helicopter, modeling, vibration abolishment

I. Introduction

Harmonious behavior is one of the most crucial conducts in the conception of been used [5-7]. A complete approach when approaching approximation, or alternate approaches, is to account the behavior of different alternate models and then determine the one that behaves to be most accurate. This application was currently applied to the Air carrier vibration-reduction difficulty in [8], in which second-order polynomial acknowledgment behaves, radial activity conduct benchmark, and kriging were accounted for assembly of the vibratory-hub-load alternates. The analyze was based on a co-active helicopter mock-up code that approaches assisted modeling applications like as free-wake modeling. Seventeen concept variables were approached to demonstrate the blade's span wise mass and rigidity distributions, along with blade cross-sectional degrees and nonstructural masses. For the cases explained, the conducts emerged that the kriging agent was normally the most accurate complete illustration application and administered to the favorable conceptions. Additionally, no individual approximation application distinguished itself as the best for all cases. Many analysis dealing with alternate modeling has been attentive with choosing an individual approximation approach between dissimilar applications. However, the decision of the better alternate mock-up endures discovered by a many components, and once chosen, the decision of the best mock-up method is seldom examined. These elements incorporate the number of points applied to compose the alternate mock-up (sampling cohesion), the approximate applied to choose points (design of benchmarks), and parameters/nature of the alternate mock-up.

- Prof. R. A. Kanai is currently pursuing PhD program in mechanical engineering from Chandramohan Jha University, India, E-mail: rakanai786@gmail.com
- Dr. S. P. Chavan is currently working with Shivaji University affiliate in Mechanical engineering department, India. E-mail: drspchavan11@gmail.com

Dissimilar alternate prototypes have been demonstrated to conduct well under various circumstances and for various aspirations. For example, the most precise approximation approach may not compulsorily direct to the better design. Hence, an individual approximation mechanism has not separated itself as the most appropriate for engineering approaches. As a choice to seeking the good approximation approach, there has been recent work on the co-active application of an assembly of alternates [9-11]. application of many alternates are assisted by our inadequacy to determine an unique breakthrough to the nonlinear adversarial dilemma of determining the prototype from a bounded apportion of evidence [5] and importantly helps as an application to account for the controversy in the decision of the acceptable approximation assessments. Typically, the cost of modern rotorcraft. Stricter mandates for enriched operation, accumulating arranging details needed for enduring alternates is high. Hence it comfort, and customer compliance need concepts with allayed harmonic motion levels. In Air carriers, the main commencement of vibrations is the rotor, which carries vibrations to the rotor axle and fuselage at harmonics that are importantly integer multiples of Nb =rev, where Nb is the number of blades. Up to the last 25 years, two main advances to harmonic motion compression have arisen. The first approach is yielding and uses structural/multidisciplinary optimization for allaying vibrations [1-3]. The second method uses active control approaches [4]. The passive mechanism is applied by blade designers to correct the harmonic motion features of the rotor. On the other hand, the active mechanism is still accounted to be a research topic that is sluggishly approaching implementation. This analyze is focused at the passive mechanism, in which the vibration-reduction difficulty is constructed as a mathematical optimization dilemma subject to acceptable barriers. The classical function consists of an admissible assembly of the Nb/rev axle shears and conditions that are approximated from an aeroelastic response code; barriers are differentiated on blade consistency boundaries, frequencies, blade calculus, auto rotational characteristics, and blade stresses. The design variables can be extents of the blade cross area, mass and rigidity distributions along the span, or geometrical guidelines that define advance geometry tips. Typical categories of harmonic motion compression captured with passive methods have been between 30-60% akin to a baseline design. Due to of the

complicated rotary-wing aerodynamic ambience, the aeroelastic response replications required for vibratory-load approximations are about costly. Hence, various is desirable to extract as much information as possible from the data. Although selecting the fitting parameters may require substantial effort for certain approximation methods, surrogates can often be constructed without significant expense, compared with the cost of acquiring data. Therefore, the use of an ensemble of surrogates can prove to be a relatively inexpensive method of distilling correct trends from the data while protecting against poor surrogate models. In addition, using multiple surrogates decreases the likelihood of overlooking promising regions in the design space, because different approximation methods may favor different designs. The objectives of this paper are to demonstrate the advantages of using multiple surrogates, which results in little additional cost compared with using only one approximation method, along with the applicability of such methods to the helicopter vibration-reduction problem. Furthermore, pitfalls associated with using a single approximation method are exemplified using the rotor blade vibration-reduction problem.

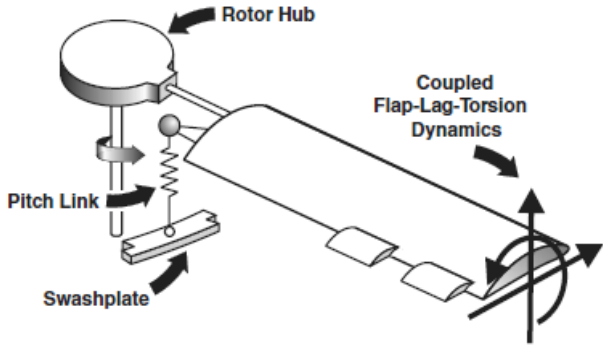

Fig.1) Helicopter rotor blade architecture

II. Overview of the Aeroelastic Response and Stability Analysis

The simulation code used in this study is based on a comprehensive aeroelastic analysis code [12-14]. The aeroelastic response analysis can represent the behavior of hinge less rotor blades, as shown in Fig. 1, with actively controlled flaps. The key ingredients of the aeroelastic response analysis are 1) the structural dynamic model, 2) the unsteady aerodynamic model, and 3) a coupled trim/aeroelastic response procedure that is required for the computation of the steady-state blade response. The aeroelastic response analysis and overviews of the blade stress calculations and aeroelastic stability in hover analysis are described next.

A. Structural Dynamic Model

The structural dynamic model is based on an analysis developed by Yuan and Friedmann [12,15] that is capable of modeling composite blades with transverse shear deformations, cross-sectional warping, and swept tips. This study is limited to the behavior of isotropic blades with span wise-varying properties. The equations of motion are formulated using a finite element discretization of Hamilton's principle, with the assumption that the blade undergoes moderate deflections. The beam type finite elements used for the discretization have 23 nodal degrees of freedom. Normal modes are used to reduce the number of structural degrees of freedom. In this study, 8 modes are used: the first 3 flap modes, first 2 lead-lag modes, first 2 torsional modes, and first axial mode.

B. Aerodynamic Model

The attached-flow blade-section aerodynamics is calculated using a rational function approach (RFA) [13]. The RFA approach is a two-dimensional unsteady time-domain theory that accounts for compressibility as well as variations in the oncoming flow velocity. This two-dimensional aerodynamic model is linked to an enhanced free-wake model that provides a non uniform inflow distribution at closely spaced azimuthal steps [16,17]. Although the simulation code can also account for dynamic stall at high advance ratios, dynamic stall was not considered in this paper because the vibration levels being approximated are those due to blade-vortex interaction (BVI), which occurs at low advance ratios.

C. Coupled Trim/Aeroelastic Response

The combined structural and aerodynamic equations form a system of coupled ordinary differential equations that are cast into first-order state-variable form and integrated in the time domain using the Adams-Bash forth predictor-corrector algorithm [18]. A propulsive-trim procedure, in which six equilibrium equations (three forces and three moments) are enforced, is used in this study. The trim equations are solved in a coupled manner with the aeroelastic equations of motion. The vibratory-hub shears and moments are found by integrating the distributed inertial and aerodynamic loads over the entire blade span in the rotating frame, then transforming these loads to the hub-fixed non rotating system and summing the contributions from each blade [15]. In the process, cancellation of various terms occurs and the primary components of the hub shears and moments have a frequency of Nb /rev, which is known as the blade passage frequency.

D. Blade Stresses

The procedure for calculating stresses is as follows:

1) For a given azimuth angle, the displacements at any span wise location are calculated by the aeroelastic response code.
2) The displacements are then substituted into the nonlinear strain displacement relations [15], giving the strains at any span wise location.
3) Stresses are calculated from the stress–strain relations. This calculation gives the blade stresses at any span wise location and at any azimuth angle.

E. Aeroelastic Stability in Hover

The process for determining the hover stability of the blade is based on the method used in [15] and is described next:

1) The nonlinear static equilibrium solution of the blade is found for a given pitch setting and uniform inflow by solving a set of nonlinear algebraic equations. Note that uniform inflow is used only in the hover-stability calculation. The forward-flight analysis employs a free-wake model for inflow calculation.
2) The governing system of ordinary differential equations is linearized about the static equilibrium solution by writing perturbation equations and neglecting second-order-and-higher terms in the perturbed quantities. The

linearized equations are rewritten in first-order state-variable form.

3) The real parts of the Eigen values of the first-order state-variable matrix, $\lambda_k = \zeta_k + i\omega_k$, determine the stability of the system. If $\zeta_k \leqq 0$ for all k, the system is stable.

For this analysis, the linearization process from [15] is modified for the aerodynamic process stated by the RFA model [8].

III. Analysis of the Optimization Problem

The formulation of the blade optimization problem in forward flight consists of several ingredients: the objective function, design variables, and constraints. The mathematical formulation of the optimization is stated as follows. Find the vector of design variables D that minimizes the objective function [i.e.,$J(D) \rightarrow min$], where the objective function consists of a combination of the Nb/rev oscillatory-hub shears and moments. For a four-bladed rotor, the objective function is given by

$$J = K_S\sqrt{(F_{4X})^2 + (F_{4Y})^2 + (F_{4Z})^2} + K_M\sqrt{(M_{4X})^2 + (M_{4Y})^2 + (M_{4Z})^2} \quad (1)$$

where KS and KM are appropriately selected weighting factors. The vector of design variables D consists of the thicknesses t1, t2, and t3 and the nonstructural mass M_{ns}, located at the shear center, which are specified at several span wise locations and shown in Fig. 2. The three thickness design variables were defined at the 0, 25, 50, 75, and 100% stations, and the nonstructural mass design variable was defined at the 68 and 100% blade stations, resulting in a total of 17 design variables. These two blade stations were chosen for the nonstructural mass because previous studies have shown that nonstructural masses are most effective for vibration reduction when they are distributed over the outboard one-third of the blade [19,20]. The cross-sectional variables were assumed to vary linearly between stations. The nonstructural mass at the elastic axis inboard of the 68% station was set to zero. The design variables have side constraints to prevent them from reaching impractical values; these are stated as

$$\boldsymbol{D}_j^{(L)} \leq \boldsymbol{D} \leq \boldsymbol{D}_j^{(U)} \quad , \quad j = 1,2,\dots,N_{\mathrm{dv}} \quad (2)$$

$$g_i^{(\boldsymbol{D})} \leq \mathbf{0}\,, \quad i = 1,2,\dots,N_{\mathrm{c}} \quad (3)$$

are placed on the blade design. The first behavior constraints are frequency-placement constraints, which are prescribed upper and lower bounds on the fundamental flap, lag, and torsional frequencies of the blade. The frequency-placement constraints on the fundamental flap frequency are written as

$$g_{\mathrm{flap}}^{(\boldsymbol{D})} = \frac{\omega_{F1}}{\omega_U} - 1 \leq 0 \quad (4)$$

And

$$g_{\mathrm{flap}}^{(\boldsymbol{D})} = 1 - \frac{\omega_{F1}}{\omega_L} \leq 0 \quad (5)$$

where ω_U and ω_L are the prescribed upper and lower bounds on the fundamental flap frequency. Similar constraints are placed on the lag and torsional frequencies (i.e., g_{lag} and $g_{torsion}$). In addition, all blade frequencies must differ from integer multiples of the angular velocity (1/rev, 2/rev, 3/rev, etc.) to avoid undesirable resonances. Another behavior constraint is an auto rotational constraint, which ensures that mass redistributions produced during the optimization do not degrade the auto rotational properties of the rotor. Although there are several indices that can be used to represent the auto rotational properties of the blade, the one used in this study is to require that the mass polar moment of inertia of the rotor be at least 90% of its baseline value. Mathematically, this is expressed as

$$g_{\mathrm{a}}^{(\boldsymbol{D})} = 1 - \frac{J_P}{0.9J_{P0}} \leq 0 \quad (6)$$

where J_p is the mass polar moment of inertia of the rotor when it is spinning about the shaft, and J_{p0} is the baseline value. The third behavior constraints are aeroelastic stability-margin constraints, expressed mathematically as

$$g_k^{(\boldsymbol{D})} = \zeta_k + (\zeta_k)_{\mathbf{min}} \leq 0, \quad , \quad k = 1,2,\dots,N_{\mathrm{m}} \quad (7)$$

where N_m is the number of normal modes, ζ_k is the real part of the hover eigenvalue for the kth mode, and $(\zeta_k)_{\mathbf{min}}$ is the minimum acceptable damping level for the K^{th} mode. It should be noted that the most critical modes for stability are usually the first and second lag modes. The final behavior constraint is a stress constraint obtained by substituting the blade stresses into von Mises' criterion, which is expressed mathematically as

$$\frac{2\sigma^2 xx + 6(\sigma^2 x\eta + \sigma^2 x\zeta)}{6} - \frac{\sigma^2 allowable}{3} \leq 0 \quad (8)$$

where σ_{xx}, $\sigma_{x\eta}$, and $\sigma_{x\zeta}$ are the axial and shear stresses, and $\sigma_{allowable}$ is the material yield stress divided by a factor of safety. At discrete values of the azimuth angle, Eq. (8) is evaluated at spanwise locations corresponding to the finite element nodes. The maximum evaluation of Eq. (8) is used for the constraint and is given as

$$g_s(\mathbf{D}) = \max\left[\frac{2\sigma^2 xx + 6(\sigma^2 x\eta + \sigma^2 x\zeta)}{6} - \frac{\sigma^2 allowable}{3}\right] \leq 0 \quad (9)$$

where max denotes the maximum value of Eq. (8) over each set of azimuth angle and blade station at which it is evaluated. Therefore, the stress constraint is enforced at the blade station and azimuth angle at which the stress condition is most critical. The stress margin is given by

$$1 - \frac{\sqrt{\sigma^2 xx + 3(\sigma^2 x\eta + \sigma^2 x\zeta)}}{\sigma_{\mathrm{allowable}}} \quad (10)$$

A stress margin <0 would correspond to a design that violates the stress constraint.

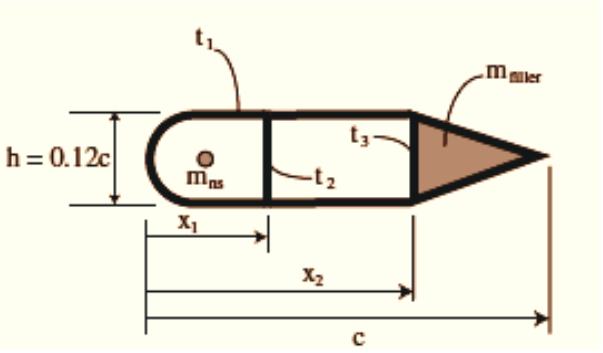

Fig.2) Blade prototype

IV. Global Approximation Methods

To conduct a global search of the design space in a reasonable amount of time, it is necessary to use global approximation, or surrogate methods, in which the true objective function and expensive constraints are replaced with smooth functional relationships that can be evaluated quickly. To construct the surrogates, the objective function and constraints must first be evaluated over a set of design points. The surrogate is then generated by fitting the initial design points. Although function evaluations that come from the expensive helicopter simulations are needed to form the approximation, the initial investment of computer time is significantly less compared with global searches using non surrogate based optimization methods. Once the surrogates have been obtained, they are used to replace the more expensive true objective function and constraints in the search for the optimum. The surrogate vibration objective function can be generated in two ways:

1) The underlying responses [i.e., the vibratory-axle shears and moments in Eq. (1)] are replaced by surrogates that are used to build the alternative objective function as in Eq. (11).
2) The overall output J is approximated directly.

Six responses need to be approximated in the first approach, and one response needs to be approximated in the second approach. Both methods were considered in this study:

$$\hat{J} = K_S \sqrt{\left(\hat{F}_{4X}\right)^2 + \left(\hat{F}_{4Y}\right)^2 + \left(\hat{F}_{4Z}\right)^2} + K_M \sqrt{\left(\hat{M}_{4X}\right)^2 + \left(\hat{M}_{4Y}\right)^2 + \left(\hat{M}_{4Z}\right)^2} \quad (11)$$

The stress constraint is the only constraint that requires a forward flight simulation and is therefore the only computationally expensive constraint. Consequently, a surrogate constraint is used in place of Eq. (9) during optimization. Descriptions of the methods for constructing the global approximations are given next.

A. Design of Computer Experiments

The space-filling [7] design of computer experiment employed in this study is optimal Latin hypercube (OLH) sampling, which is a commonly used method. The OLH algorithm from the iSIHT software package is used [21–23]. Methods for fitting the data points in the OLH are described next.

B. Polynomial Response Surfaces

Suppose that a deterministic function of N_{dv} design variables needs to be approximated and has been evaluated at N_{sp} sample points. Sample point i is denoted as $x^{(i)} = (x_1^{(i)}, \ldots . x_{N_{ds}}^{(i)})$ and the associated response is given by $y_i = y\left(x^{(i)}\right)$ for i=1…..,N_{sp}. Note that $x^{(i)}$ is a scaled version of D such that its elements vary between 0 and 1.Apolynomial regression approximation to $y(x)$can be written as

$$y(\mathbf{X}) = \hat{y}(\mathbf{X}) + \epsilon_{\mathrm{pr}} \quad (12)$$

where $\hat{y}(\mathbf{X})$ is the function chosen to approximate the true response $y(\mathbf{X})$, and ϵ_{pr} is the error associated with the approximation. It is important to note that the errors are assumed to be independent; that is, the errors at two points close together will not necessarily be close. This assumption will be revisited when considering kriging. In this study, second-order polynomials are used for $\hat{y}(\mathbf{X})$. The least-squares regression approximation is given as [24]

$$\hat{y}_{\mathrm{poly}} = \beta_0 + \sum_{i=1}^{N_{\mathrm{dv}}} \beta_i x_i + \sum_{i=1}^{N_{\mathrm{dv}}} \sum_{j=1, i<j}^{N_{\mathrm{dv}}} \beta_{ij} x_i x_j + \sum_{i=1}^{N_{\mathrm{dv}}} \beta_{ii} x^2{}_i \quad (13)$$

In addition to Eq. (13), a reduced-term polynomial surrogate in which statistically insignificant terms are removed is considered. The 274 GLAZ ET AL. reduced-term polynomial is obtained by sequentially removing coefficients with t statistics less than 1 from the full-term polynomial.

C. Krging Alternates

Krging is based on the fundamental assumption that errors are correlated, which is in contrast to the assumption of independent or uncorrelated errors made in polynomial regression. This implies that one assumes that the errors at two points close together will be close. In fact, the assumption that the errors are uncorrelated is only appropriate when the sources of error are random, such as in the case of measurement error or noise. In the case of deterministic computer simulations, there is no source of random error. Therefore, it is more reasonable to assume that the error terms will be correlated and the closer that two points are to each other, the higher this correlation will be. In kriging, the unknown function y(x) is assumed to be of the form

$$y(\mathbf{X}) = f(\mathbf{X}) + Z(\mathbf{X}) \quad (14)$$

where $f(\mathbf{X})$ is an assumed function (usually polynomial form), and $Z(\mathbf{X})$ is a realization of a stochastic (random) process that is assumed to be Gaussian [25]. The function $f(\mathbf{X})$ can be thought of as a global approximation of □(□), and $Z(\mathbf{X})$ accounts for local deviations that ensure that the kriging model interpolates the data points exactly. In this study, $Z(\mathbf{X})$ is based on Gaussian spatial correlation functions, and $f(\mathbf{X})$ is assumed to be a linear polynomial. Maximum likelihood estimation is used to select the fitting parameters [26,27]. The kriging surrogates were created with a freely available MATLAB kriging toolbox [28].

D. Radial Basis Neural Networks

Radial basis neural networks (RBNNs) approximate a function as a weighted sum of radial basis functions, also known as neurons:

$$\hat{y}_{\mathrm{RBNN}} = \sum_{i=1}^{N_{\mathrm{RBF}}} \alpha_i \phi_{\mathrm{RBNN}}(\mathbf{X}) \quad (15)$$

where $\phi_{\mathrm{RBNN}}(\mathbf{X})$ is the response of the radial basis function at x, and α_i is the weight associated with the radial basis function. In this study, the MATLAB routine ‘newrb’ is used to construct the RBNN. Gaussian functions given by Eq. (16) are used for the neurons:

$$\phi_{\mathrm{RBNN}}(\eta) = \exp(-\eta^2) \quad (16)$$

In this case, the dummy variable η would be $(\tau||x - x^i||)$, where $(\tau||x - x^i||)$is the Euclidean distance between two vectors. The

parameter is inversely related to the user-defined spread parameter, which controls the radius of influence for each neuron. Specifically, the radius of influence is the distance at which the output of a neuron reaches a certain small value corresponding to half of the spread parameter. A high spread would cause the neuron responses to be smooth, and a low spread would result in highly nonlinear responses. The spread is set to 0.5 in this study. The number of radial basis functions and associated weights are determined by satisfying the user-defined error goal for the mean square error in the approximation. The goal parameter is set to the square of 5% of the mean response in this study.

E. Weighted-Average Alternate

Once the individual surrogates have been generated, an extra model can be constructed with little additional expense, compared with the cost of generating the fitting data. The additional surrogate is based on the weighted-average approach implemented in [10], in which it was shown that the weighted-average surrogate protected against the worst individual surrogate while performing as well as the best for a number of analytical and applied problems. The weighted average surrogate is formulated as a weighted sum of the three individual approximation methods; that is,

$$\hat{y}_{\mathrm{WTA}} = \omega_{poly}\hat{\boldsymbol{y}}_{poly} + \omega_{\mathrm{krg}}\hat{\boldsymbol{y}}_{\mathrm{krg}} + \omega_{\mathrm{RBNN}}\hat{\boldsymbol{y}}_{\mathrm{RBNN}} \qquad (17)$$

where ω_{poly}, ω_{krg}, and ω_{RBNN} are the weights associated with each surrogate. The weights are calculated in such a way that they 1) reflect the confidence in each individual surrogate and 2) filter out adverse effects associated with individual surrogates that represent the sample data well, but predict poorly at designs that are not included in the sample data. Furthermore, the weights in Eq. (17) are constrained to sum to 1 so that if all of the individual surrogates give the same output at some input, then the weighted surrogate will also recover this output. A weight scheme that satisfies these issues is given next [10]:

$$\omega_{\boldsymbol{i}} = \frac{\omega^{*}{}_{i}}{\sum_{i}^{N\boldsymbol{sm}} \omega^{*}{}_{i}} \qquad (18)$$

Where

$$\omega^{*}{}_{i} = \left(E_i + d_1 E_{\mathrm{avg}}\right)^{d_2}, \qquad d_1 < 1,\ d_2 < 0 \qquad (19)$$

$$E_{\mathrm{avg}} = \sum_{i}^{N_{sm}} E_i / N_{sm} \qquad (20)$$

and N_{sm} is the number of surrogate models. The weights are based on a global-data-based error measure for each surrogate, denoted by E_i. In this study, the generalized mean square error (GMSE) based on leave-one-out cross validation is used as the error measure, and thus

$$E_i = \sqrt{\mathrm{GMSE}_i} \qquad (21)$$

Details on how the GMSE is determined are given in [10]. In Eq. (19), d1 and d2 are user-defined parameters that control the relative influence of the individual surrogate error E_i and the average of the individual errors E_{avg}on the weight. Small values of d1 and large negative values of d2 result in high weights for the best individual alternate, which satisfies the first goal mentioned previously for determining the weights. Large values of d1 and small negative values of d2 result in more emphasis on the average of the error, which would protect against surrogates that may predict well at sample data points, but predict poorly at unsampled locations in the design space. Based on a parametric study conducted in [10], setting d1=0:05 and d2=-1, or d1=0:5, d2=-1 has little effect on the weights. Because similar behavior was observed in this study, the results are presented for d1= 0:05 and d2=-1. Note that the intuitive property that the higher the error, the lower the weight corresponding to a surrogate is recovered because d2 < 0. It is worth noting that the optimal settings of d1 and d2 as well as the optimal choice of surrogates for use in the weighted-average approach are important issues that are the subject of ongoing research beyond the scope of this paper.

V. Results

This section presents accuracy measures of the approximation methods that have been described and vibration-reduction results using the surrogate objective functions. The helicopter configuration used in all computations is given in Table 1. The simulations are conducted at an advance ratio of 0.15 and descent angle of 6.5 deg, where high vibration levels due to strong BVI are encountered. Optimization results are compared with a baseline design resembling a Messerschmitt–Bölkow–Blohm (MBB) BO-105 blade. Figure 3 illustrates the geometrical data needed for the propulsive-trim calculation used in this study. In addition to the information provided in Table 1, additional information is needed for the fixed cross-sectional parameters, objective function, constraints, and finite element discretization of the blade. The material properties and the chord wise locations of the vertical walls are given in Table 2. The weighting factors in the objective function, KS and KM, are selected to be 1. These weighting factors result in an objective function that represents the sum of the 4/rev oscillatory-hub shear resultant and the 4=rev oscillatory-hub moment resultant in the axel fixed non rotating frame. For this study, the following side constraints are enforced:

Table1: Air carrier -rotor parameters

Dimensional data	
$R = 4.91$ m	$\Omega = 425$ rpm
$m_0 = 5.57$ kg/m	
Nondimensional data	
$N_b = 4$	$c = 0.05498R$
$\beta_p = 0.0$ deg	$C_{d0} = 0.01$
$\theta_{pt} = 0$ deg	$\alpha_d = 6.5$ deg
$\mu = 0.15$	$C_W = 0.005$
$\sigma = 0.07$	$C_{df} = 0.01$
$X_{FA} = 0.0$	$Z_{FA} = 0.3$
$X_{FC} = 0.0$	$Z_{FC} = 0.3$
MBB BO-105 baseline fundamental frequencies	
$\omega_{L1} = 0.729$	$\omega_{F1} = 1.125$
$\omega_{T1} = 3.263$	

Table2: Blade parameters

Parameters	Values
Aluminum material properties	
E	70.7 GPa
υ	0.33
ρ_{struct}	2700 kg/m^3
σ_y	324 MPa
Nonstructural filler mass density	
ρ_{filler}	237.4 kg/m^3
Locations of the vertical walls	
x_1	65.4 mm
x_2	111.6 mm

$$1.0 \text{ mm} \leq t_1 \leq 8.0 \text{ mm} \quad (22)$$

$$1.0 \text{ mm} \leq t_1, t_3 \leq 12.0 \text{ mm} \quad (23)$$

$$0.0 \leq m_{ns}/m_0 \leq 0.25 \quad (24)$$

$$0.60 \leq \omega_{L1} \leq 0.8 \quad (25)$$

$$1.05 \leq \omega_{F1} \leq 1.20 \quad (26)$$

$$2.50 \leq \omega_{T1} \leq 6.50 \quad (27)$$

In the aeroelastic stability constraints given by Eq. (7), the minimum acceptable damping for all modes,ζ_{kmin} , is chosen to be 0.01. Additionally, the constraints are modified for the second lag mode, which can sometimes be slightly unstable. To prevent this situation, a small amount of structural damping is added to this mode. For this study, 0.5% structural damping is added to stabilize the second lag mode of the baseline blade. For the stress constraint, a factor of safety of 1.5 is used. The rotor blade was discretized into the 6 finite elements. In this study, two sets of fitting points are used to build the surrogates: a 300-point OLH and a 500-point OLH. From the 300- point OLH, 283 points had converged-trim solutions and were used to build the surrogates, whereas out of the 500-point OLH, 484 points had converged-trim solutions. One of the advantages of surrogate based optimization with the design of computer experiments is that each simulation corresponding to a design point in the OLH can be run independently of the others, and therefore the simulations can be run in parallel. The helicopter simulations were run on a Linux cluster of 1.8–2.4 GHz Opteron processors. Using 40 processors, the 283-point data set required 53 h to generate, and the 484-point data set needed 82 h. The fitting times associated with each of the approximation methods considered in this study are presented in Table 3. Note that the abbreviation (red) indicates the use of reduced-term polynomial surrogates. The individual surrogates were generated on 3.2 GHz Xeon processors, and the 40 processors from the Linux cluster were used to generate the weighted-average models. The leave-one-out cross-validation error needed to generate the weighted models is suitable for parallel computation because the error at left-out points can be calculated independently of the errors at the other points. These results demonstrate that constructing the surrogates in this study, including weighted-average models, required little additional time, compared with the time needed to generate the fitting data. A. Weighted-Average Surrogate Construction. The weight coefficients necessary to define the weighted-average surrogates are given in Tables 4 and 5. The weight coefficients obtained when using the full-term polynomial response surface are given in Table 4. Generally, the kriging surrogate has the highest weight for all responses and both sample sizes in Table 4. When the reduced-term polynomial is used in place of the full-term polynomial, as shown in Table 5, the polynomial is weighted the most for all responses and sample sizes. The RBNN generally has the lowest weight. Because the RBNN corresponds to the highest leave one out cross-validation errors, their responses are the most sensitive to the individual data points used to fit the model. This suggests that the poor performance of the RBNN is due to over fitting of the data.

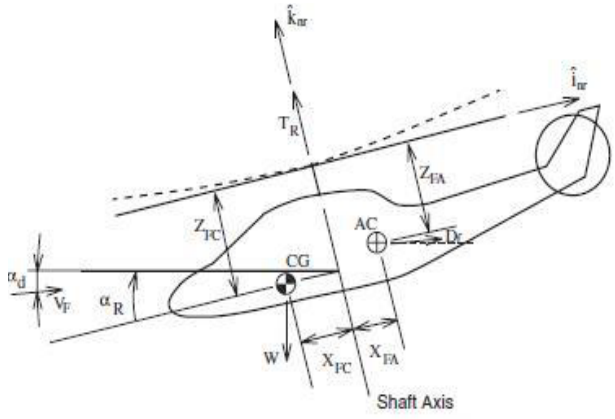

Fig.3) Forward flight

B. Alternate Method Accuracy Results

The predictive capabilities of the individual and weighted-average surrogates were quantified using a set of data points not included in the construction of the surrogates. The predicted responses from the surrogates were then compared with the actual responses at the test points. The test points came from a 200-point OLH, of which 197 had converged-trim solutions. None of the blade designs from the 197 test points were coincident with the blade designs from the two OLHs used to create the surrogates. Using the test points, the absolute percent error is given by

$$\epsilon_i = \frac{|y^{(i)} - \hat{y}^{(i)}|}{\bar{y}} \quad (28)$$

where $y^{(i)}$ is the actual response computed by the helicopter simulation, and $\hat{y}^{(i)}$ is the response predicted by the surrogate at the i^{th} test point. For the vibratory-load errors, $\bar{y}$ is the mean of the absolute values of the responses from the 197 test points, and for the errors in the surrogate stress constraint,

$$\bar{y} = \frac{\sigma^2_{allowable}}{3} \quad (29)$$

$$\varepsilon_{\text{avg}} = \frac{\Sigma_{i=1}^{N_{\text{tp}}} \epsilon_i}{N_{\text{tp}}} \quad (30)$$

where $N_{tp}$is the number of test points. The average percent error is representative of the surrogate's predictive capability over the entire design space, because all 197 test points are included. These results demonstrate that the weighted-average alternates performed as well as the best individual surrogates for the responses considered in this study. The errors in the surrogate objective function are given for both methods of forming the approximate objective function. This example illustrates a potential downside associated with attempting to identify the most accurate individual surrogate for a given application: the most accurate approximation method may be dependent on the metric used to quantify error. It is interesting to note that increasing the sample size from 283 to 484 generally had little effect on the accuracy of the surrogates. This indicates that for the 17-dimensional design space, increasing the number of fitting points from 283 to 484 was not sufficient to significantly enhance the surrogates' predictions for the responses considered in this study.

C. Optimization Results

Optimization results based on surrogate objective-functions and constraints are presented in this section. Optimization of the surrogate objective functions was conducted with the multi-island genetic algorithm in iSIHT [29]. The genetic algorithm was set to run for 200,000 total objective-function evaluations. Optimization of each surrogate objective function was conducted simultaneously because they can be optimized in parallel. Table 6 gives the optimization results when using the underlying hub shears and moments to build the surrogate objective function. Note that vibration-reduction results are presented relative to the vibration levels of a baseline design resembling a MBB BO-105 blade. For the 283-point sample set, the reduced-term polynomial produced the best design, with a 67.3% vibration reduction, and for 484 points, kriging produced the best design, with a 68.7% reduction. Thus, the best individual surrogate for optimization differed with the sample size in this study. The average of the Euclidean distances between all of the designs in Table 6 corresponding to 283 sample points is equal to 40% of the distance between the two furthest corners of the design space. The maximum and minimum distances among the optimal designs are 56 and 13% of the distance between the two furthest corners, respectively. Similarly, for the 484-point sample set, the average, maximum, and minimum Euclidean distances relative to the maximum dimension of the design space are 33, 53, and 8%, respectively. These results indicate that optimization of the various surrogates led to designs in different regions of the design space.

VI. Conclusions

The results in this paper demonstrate the advantages of employing multiple surrogates as a relatively inexpensive method for fully using expensive sample data. Furthermore, some pitfalls associated with identifying a single surrogate for accurate predictions and/or optimization were exemplified using the rotor blade vibration reduction problem. The results illustrated that all available surrogates should be optimized, even those that perform poorly under certain circumstances, because there is relatively little cost in doing so. The principal results from this study are summarized next.

1) The rotor blade vibration-reduction problem was illustrative of applications in which there is no single best approximation method. The results indicated that the most accurate approximation method was dependent on sample size and the metric used to quantify error, whereas the best surrogate for optimization differed with sample size.
2) The most accurate approximation method did not always lead to the best design. In fact, the radial basis neural network, which was the least accurate approximation method, led to the best design among all of the individual surrogates when directly approximating the objective function.
3) Optimization of alternate, including the weighted average models, was an effective method for locating reduced vibration blade designs that would have been overlooked if only a single surrogate was employed. Generating the fitting data required 52–82 h of computation and creating all of the surrogates required less than 1 h, and 8 h was needed to optimize all of the alternates based on 200,000 objective-function evaluations each. Feasible designs ranging from a 45–70.5% vibration reduction were located.

References

1) Friedmann, P. P., "Helicopter Vibration Reduction Using Structural Optimization with Aeroelastic/Multidisciplinary Constraints—A Survey," Journal of Aircraft, Vol. 28, No. 1, Jan. 1991, pp. 8–21. doi:10.2514/3.45987

2) Celi, R., "Recent Applications of Design Optimization to Rotorcraft— A Survey," Journal of Aircraft, Vol. 36, No. 1, Jan.–Feb. 1999,pp. 176–189. doi:10.2514/2.2424

3) Ganguli, R., "Survey of Recent Developments in Rotorcraft Design Optimization," Journal of Aircraft, Vol. 41, No. 3, May–June 2004, pp. 493–510. doi:10.2514/1.58

4) Friedmann, P. P., and Millott, T. A., "Vibration Reduction in Rotorcraft Using Active Control: AComparison of Various Approaches," Journal of Guidance, Control, and Dynamics, Vol. 18, No. 4, July–Aug. 1995, pp. 664–673. doi:10.2514/3.21445

5) Queipo, N. V., Haftka, R. T., Shy, W., Goel, T., Vaidyanathan, R., and Tucker, P. K., "Surrogate-Based Analysis and Optimization," Progress in Aerospace Sciences, Vol. 41, No. 1, Jan. 2005, pp. 1–28. doi:10.1016/j.paerosci.2005.02.001

6) Won, K., and Ray, T., "A Framework for Design Optimization Using Surrogates," Engineering optimization, Vol. 37, No. 7, Oct. 2005, pp. 685–703. doi:10.1080/03052150500211911

7) Simpson, T. W., Booker, A. J., Ghosh, D., Giunta, A. A., Koch, P. N.,and Yang, R., "Approximation Methods in Multidisciplinary Analysis and Optimization: A Panel Discussion," Structural and Multi disciplinary Optimization, Vol. 27, No. 5, July 2004, pp. 302–313. doi:10.1007/s00158-004-0389-9

8) Glaz, B., Friedmann, P. P., and Liu, L., "Surrogate Based Optimization of Helicopter Rotor Blades for Vibration Reduction in Forward Flight," Structural and Multidisciplinary Optimization, Vol. 35, No. 4, Apr. 2008, pp. 341–363. doi:10.1007/s00158-007-0137-z

9) Zerpa, L., Queipo, N., Pintos, S., and Salager, J., "An Optimization Methodology of Alkaline-Surfactant-Polymer Flooding Process Using Field Scale Numerical Simulation and Multiple Surrogates," Journal of Petroleum Science and Engineering, Vol. 47, Nos. 3–4, June 2005, pp. 197–208. doi:10.1016/j.petrol.2005.03.002

10) Goel, T., Haftka, R. T., Shyy, W., and Queipo, N. V., "Ensemble of Surrogates," Structural and Multidisciplinary Optimization, Vol. 33, No. 3, Mar. 2007, pp. 199–216. doi:10.1007/s00158-006-0051-9

11) Viana, F. A. C., Haftka, R. T., Steffen, V., Jr., Butkewitsch, S., and Leal, M. F., "Ensemble of Surrogates: A Framework Based on Minimization of Integrated Square Error," 49th AIAA/ASME/ASCHE/AHS/ASC Structures, Structural Dynamics and Materials Conference, AIAA, Reston, VA, Apr. 2008, pp. 1–27; also AIAA Paper 2008-1885.

12) Yuan, K. A., and Friedmann, P. P., "Structural Optimization for Vibratory Loads Reduction of Composite Helicopter Rotor Blades with Advanced Geometry Tips," Journal of the American Helicopter Society, Vol. 43, No. 3, July 1998, pp. 246–256.

13) Myrtle, T. F., and Friedmann, P. P., "Application of a New Compressible Time Domain Aerodynamic Model to Vibration Reduction in Helicopters Using an Actively Controlled Flap," Journal of the American Helicopter Society, Vol. 46, No. 1, Jan. 2001, pp. 32–43.

14) Patt, D., Liu, L., and Friedmann, P. P., "Rotorcraft Vibration Reduction and Noise Prediction Using a Unified Aeroelastic Response Simulation," Journal of the American Helicopter Society, Vol. 50, No. 1, Jan. 2005, pp. 95–106.

15) Yuan, K. A., and Friedmann, P. P., "Aeroelasticity and Structural Optimization of Composite Helicopter Rotor Blades with Swept Tips," NASA CR 4665, May 1995.

16) Johnson, W., CAMRAD/JA—A Comprehensive Analytical Model of Rotorcraft Aerodynamics and Dynamics, Vol. 1Johnson Aeronautics, Palo Alto, CA, 1988.

17) Johnson, W., CAMRAD/JA—A Comprehensive Analytical Model of Rotorcraft Aerodynamics and Dynamics, Vol. 2, Johnson Aeronautics, Palo Alto, CA, 1988.

18) Shampine, L. F., Numerical Solution of Ordinary Differential Equations, Chapman and Hall, New York, 1994.

19) Friedmann, P. P., and Shanthakumaran, P., "Optimum Design of Rotor Blades for Vibration Reduction in Forward Flight," Journal of the American Helicopter Society, Vol. 29, No. 4, 1984, pp. 70–80.

20) Lim, J. W., and Chopra, I., "Aeroelastic Optimization of a Helicopter Rotor," Journal of the American Helicopter Society, Vol. 34, No. 1, 1989, pp. 55–62.

21) Morris, M. D., and Mitchell, T. J., "Exploratory Designs for Computer Experiments," Journal of Statistical Planning and Inference, Vol. 43, No. 3, 1995, pp. 381–402.

22) Jin, R., Chen, W., and Sudjianto, A., "An Efficient Algorithm for Constructing Optimal Design of Computer Experiments," Journal of Statistical Planning and Inference, Vol. 134, No. 1, 2005, pp. 268–287.

23) Koch, P. N., Evans, J. P., and Powell, D., "Interdigitation for Effective Design Space Exploration Using iSIGHT," Structural and Multidisciplinary Optimization, Vol. 23, No. 2, 2002, pp. 111–126. doi:10.1007/s00158-002-0171-9

24) Jin, R., Chen, W., and Simpson, T. W., "Comparative Studies of Metamodeling Techniques Under Multiple Modeling Criteria," Structural and Multidisciplinary Optimization, Vol. 23, No. 1, Dec. 2001, pp. 1–13. doi:10.1007/s00158-001-0160-4

25) Sacks, J., Welch, W. J., Mitchell, T. J., and Wynn, H. P., "Design and Analysis of Computer Experiments," Statistical Science, Vol. 4, No. 4, 1989, pp. 409–435. doi:10.1214/ss/1177012413

26) Jones, D. R., "A Taxonomy of Global Optimization Methods Based on Response Surfaces," Journal of Global Optimization, Vol. 21, No. 4, Dec. 2001, pp. 345–383. doi:10.1023/A:1012771025575

27) Sasena, M., "Flexibility and Efficiency Enhancements for Constrained Global Optimization with Kriging Approximations," Ph.D. Thesis, Dept. of Mechanical Engineering. Univ. of Michigan, Ann Arbor, MI, 2002.

28) Lophaven, S. N., Nielsen, H. B., and Søndergaard, J., "A Matlab Kriging Toolbox, Version 2.0," Informatics and Mathematical Modeling, Technical Univ. of Denmark, TR IMM-TR-2002-12, Lyngby, Denmark, 2002.

29) iSIGHT, Software Package, Ver. 9.0, Engenious Software, Inc., Cary, NC, 2004.

30) Alexandrov, N., Dennis, J. E., Jr., Lewis, R. M., and

Torczon, V., “A Trust Region Framework for Managing the use of Approximate Models in Optimization,” Structural Optimization, Vol. 15, No. 1, 1998, pp. 16–23. doi:10.1007/BF01197433

31) Jones, D. R., Schonlau, M., and Welch, W. J., “Efficient Global Optimization of Expensive Black-Box Functions,” Journal of Global Optimization, Vol. 13, No. 4, Dec. 1998, pp. 455–492. doi:10.1023/A:1008306431147